A New Technique to Measure Infiltration rate for Assessing Infiltration of BMPs

F. Ahmed[*], J. S. Gulliver[**] and J. L. Nieber[***],

[*]*St Anthony Falls Laboratory, Department of Civil Engineering, University of Minnesota, #2 third avenue SE, Minneapolis, MN55414, 612-624-4629, email: ahmed262@umn.edu*
[**]*Department of Civil Engineering, University of Minnesota, Minneapolis, MN55414, 612-625-4080, email: gulli003@umn.edu*
[***]*Department of Bioproducts and Biosystems Engineering, University of Minnesota, St. Paul, MN 55108, 612-625-6724, email: nieber@umn.edu*

ABSTRACT
Infiltration is an essential process of most stormwater best management practices and measurements of the infiltration rate applied to a design storm are needed to determine performance, schedule maintenance and meet regulatory requirements. Infiltration rates, however, have great spatial variation, and infiltration measurement techniques are relatively slow. The Modified Philip-Dunne (MPD) infiltrometer is a new technique to measure the saturated hydraulic conductivity (K_{sat}) of surface soil. It is a fast, simple and inexpensive falling head device; suitable for infiltration practices because it can be performed relatively quickly to capture the large spatial variability that occurs with infiltration rates. A user-friendly spreadsheet program and a manual have made the application of the MPD infiltrometer straight-forward so that the infiltration rate of soil can be obtained quickly. A comparison between the value of K_{sat} obtained from MPD and from the numerical simulations of the Richards equation for homogeneous and non-homogeneous soil will be presented.

KEYWORDS
Infiltration, storm water best management practice, saturated hydraulic conductivity, hmogeneous and nonhomogeneous soil.

INTRODUCTION
For most stormwater infiltration practices, i.e., bioretention facilities, infiltration basins, swales and filter strips, infiltration is the primary means to remove pollutants and to delay peak stormwater flow. But; because of the accumulation of fine particle on the soil surface and the use of heavy equipment during construction which results in reduced pore volume of the soil surface; leads to reduced infiltration capacity of that infiltration practice. So, measuring the hydraulic characteristics of the soils in the infiltration practices facilitates the ability to assess the infiltration response of these constructed practices to design storm events, and to schedule and plan maintenance to meet regulatory requirements.

The most common devices used to determine the infiltration capacity of soil are the single and double ring infiltrometers (Ashraf et al., 1997; Dirk et al., 1999; Ben-Hur and Assouline, 2002). These devices are time consuming, require large volumes of water to perform the test and more than one test cannot be performed simultaneously since these are constant head test.

But in an infiltration practice the saturated hydraulic conductivity (K_{sat}) of soil can vary spatially by two orders of magnitude range (Asleson et al., 2009). At the same location K_{sat} can also change over time. These changes can be due to compaction, loss of soil structure, freezing and thawing cycles, and clogging. For these reasons it is important to take a significant number of infiltration measurements in the infiltration practice because one measurement will have a great uncertainty associated with it. To capture the spatial variability of the hydraulic conductivity of soil (Asleson et al., 2009) and to determine a representative infiltration capacity, a large number of measurements are needed. The Modified Philip Dunne (MPD) Infiltrometer is a new falling head device that can be used to measure the infiltration capacities at up to 20 locations simultaneously to estimate a representative infiltration capacity. It is an adaptation, modification of the original Philip-Dunne borehole infiltrometer (Philip, 1993). This device is currently being used to characterize the infiltration properties of swales and has been used extensively to characterize the infiltration properties of several LID best management practices, such as bioretention facilities and infiltration basins.

In this paper the background of the MPD infiltrometer will be discussed, a comparison between MPD infiltrometer and double ring infiltrometer both experimentally and numerically for homogeneous and nonhomogeneous soil will also be discussed.

METHODS

Modified Philip Dunne (MPD) Infiltrometer

The MPD is an open ended cylinder of 10cm diameter which consists of two parts: the top part is 37cm long constructed of clear PVC pipe and the detachable bottom part is 7cm long made of finished steel. An O-ring keeps the seal between the two parts tight. If the ground is dry and hard, the MPD has to be pounded into the ground using a rubber mallet and a fitted hammering plate. A metric measuring tape is adhered to the outside of the clear PVC pipe to allow measurement of the water level over time with a stop-watch for each infiltrometer.

Figure 1: Modified Philip-Dunne Infiltrometer

Initial volumetric soil moisture content measurements need to be made around the device (Klute, 1986) or estimated by some method. The typical effective porosity of that type of soil is also need to be known. After the MPD has been pounded into the ground it has to be filled with water up to a predetermined height and then the height of water level inside the MPD is recorded with time. A stop watch is used to record the time. The saturated moisture content is derived from the porosity of the soil. Using the software developed by St. Anthony Falls Laboratory (Asleson et al., 2009; Ahmed and Gulliver, 2010), the recordings of the water drop together with the initial and final moisture content in the soil can be used to calculate values for K_{sat} and wetting front suction.

The original Philip Dunne permeameter involved placing the device inside a borehole (Philip, 1993; Munoz-Carpena, 2002), but the MPD infiltrometer incorporates surface infiltration and therefore will capture the effect of sediment accumulation or surface compaction for an infiltration practice.

Theory of the Modified Phillip-Dunne Infiltrometer

The mathematical model of the MPD infiltrometer is a modification of Philip's borehole permeameter model (Philip 1993). Assumptions that were made are: isotropic homogeneous

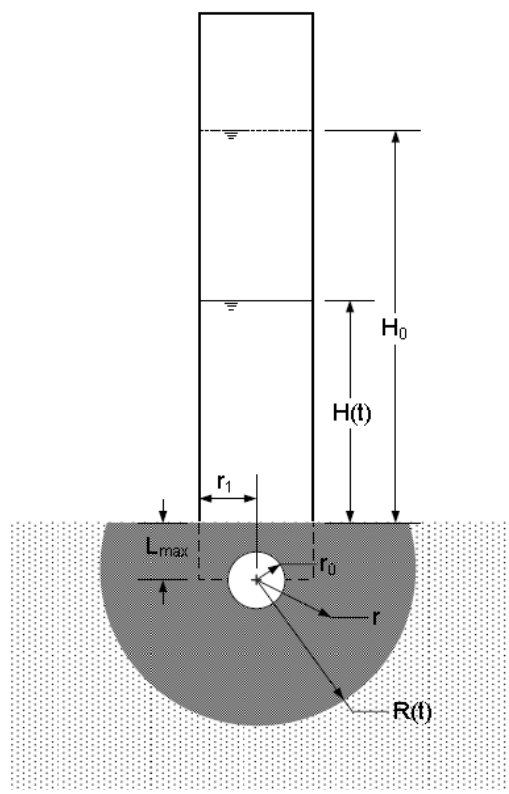

Fig 2: Important parameters of the MPD infiltrometer. H_0 is the initial height of water; $H(t)$ is the height of water at time t; L_{max} is the depth of insertion into the soil; r_0 is the equivalent source radius; r_1 is the radius of the cylinder; r, any radius within the wetted front; and $R(t)$ is the radius to the sharp wetted front at time t.

media, a Green-Ampt sharp wetting front and a spherical geometry for the wetting front by subtracting the gravitational component of the flow. The equation for cumulative infiltration assuming capped sphere as shown in Figure 1, is:

$$i(t) = \frac{\pi}{3}(\theta_f - \theta_i)\left(2R(t)^3 + 3R(t)^2 L_{\max} - L_{\max}^3 - 4r_0^3\right) \quad \text{..... (1)}$$

where θ_f and θ_i are the final and initial moisture content of the soil. Following the same analysis procedure as Philip (1993), the pressure capillary potential drop ΔP from the spherical source to the wetted front becomes (Nestingen, 2007):

$$\Delta P(t) = \frac{\pi^2}{8}\left\{\left(\theta_f - \theta_i\right)\frac{R(t)^2 + R(t)L_{\max}}{K_{sat}}\frac{dR}{dt} - 2r_0^2\right\}\frac{\ln\left[\frac{R(t)\left(r_0 + L_{\max}\right)}{r_0\left(R(t) + L_{\max}\right)}\right]}{L_{\max}} \quad \text{..... (2)}$$

The pressure capillary potential drop from the spherical source to the wetted front using Darcy's law would be (Nestingen, 2007):

$$\Delta P(t) = C - H(t) - L_{\max} + \frac{L_{\max}}{K_{sat}}\frac{dH}{dt} \quad \text{..... (3)}$$

where K_{sat} is the saturated hydraulic conductivity and C is the wetting front suction. From equation (2) and (3) we get the following equations:

$$dH = \frac{K_{sat}}{L_{\max}}\left[\frac{\pi^2}{8}\left\{\left(\theta_f - \theta_i\right)\left(\frac{R(t)^2 + R(t)L_{\max}}{\overline{K}_{sat}}\frac{dR}{dt}\right) - 2r_0^2\right\}\frac{\ln\left\{\frac{R(t)(r_0 + L_{\max})}{r_0(R(t) + L_{\max})}\right\}}{L_{\max}} - C + H + L_{\max}\right]dt \quad \text{.... (4)}$$

$$dt = \frac{\frac{\pi^2}{8}\left(\theta_f - \theta_i\right)\frac{R(t)^2 + R(t)L_{\max}}{K_{sat}L_{\max}}\ln\left\{\frac{R(t)\left(r_0 + L_{\max}\right)}{r_0\left(R(t) + L_{\max}\right)}\right\}dR - \frac{L_{\max}}{\overline{K}_{sat}}dH}{C - H(t) - L_{\max} + \frac{\pi^2}{4}\frac{r_0^2}{L_{\max}}\ln\left\{\frac{R(t)\left(r_0 + L_{\max}\right)}{r_0\left(R(t) + L_{\max}\right)}\right\}} \quad \text{..... (5)}$$

The discretized form of equation (4) and (5) are as follows:

$$H_i^{n+1} - H_i^n = \frac{K_{sat}}{L_{\max}}\left[\frac{\pi^2}{8}\left\{\left(\theta_f - \theta_i\right)\left(\frac{R_i^{n+1^2} + R_i^{n+1}L_{\max}}{K_{sat}}\frac{(R_i^{n+1} - R_i^n)}{\Delta t}\right) - 2r_0^2\right\}\frac{\ln\left\{\frac{R_i^{n+1}(r_0 + L_{\max})}{r_0(R_i^{n+1} + L_{\max})}\right\}}{L_{\max}} - C + H_i^n + L_{\max}\right]\Delta t \quad \text{..... (6)}$$

$$T_i^{n+1} - T_i^n = \frac{\frac{\pi^2}{8}\left(\theta_f - \theta_i\right)\frac{R_i^{n+1^2} + R_i^{n+1}L_{\max}}{K_{sat}L_{\max}}\ln\left\{\frac{R_i^{n+1}\left(r_0 + L_{\max}\right)}{r_0\left(R_i^{n+1} + L_{\max}\right)}\right\}(R_i^{n+1} - R_i^n) - \frac{L_{\max}}{K_{sat}}\Delta H}{C - H_i^{n+1} - L_{\max} + \frac{\pi^2}{4}\frac{r_0^2}{L_{\max}}\ln\left\{\frac{R_i^{n+1}\left(r_0 + L_{\max}\right)}{r_0\left(R_i^{n+1} + L_{\max}\right)}\right\}} \quad \text{..... (7)}$$

For more accuracy in the computation of K_{sat} and C the middle points between two consecutive observed head vs time data was interpolated using cubic spline approximation (Hanna and Sandall, 1995). Equation (6) and the interpolated midpoint head difference were used to determine the value of K_{sat} and C, again equation (7) and the interpolated midpoint time difference were also used to determine the value of K_{sat} and C. The solution is achieved by minimizing the root mean square (rms) of the difference between interpolated head increment and predicted head increment (dH) and interpolated time increment and predicted

time increment (dt), by adjusting the values of saturated hydraulic conductivity (K_{sat}) and soil suction (C). The better of the two curve fits is used as the optimized K_{sat} and C.

Field Test

In our study the MPD infiltrometer and the double ring infiltrometer (DRI) were installed at the same location of an infiltration basin 1.5m apart from each other and two tests were performed simulataneously to calculate the K_{sat}. The infiltration basin is located in the south east of Minnesota. The area of the infiltration basin was about 0.55 ha and it is a well-vegetated basin with a soil type of mostly silty loam to clay. The MPD infiltrometer and DRI were used to calculate the K_{sat} of the soil at 5 different locations of this basin.

Computational Model

A numerical commercial software program (COMSOL, 2010) which can solve Richards equation for the three-dimensional axisymmetric conditions was used to evaluate how well the MPD and DRI represent the infiltration properties of a soil. The assumed equation is the three-dimensional axisymmetric equation given by

$$\frac{\partial \theta}{\partial t} = \frac{1}{r}\frac{\partial}{\partial r}\left(Kr\frac{\partial h}{\partial r}\right) + \frac{\partial}{\partial z}\left(Kr\frac{\partial h}{\partial z}\right) + \frac{\partial K}{\partial z}$$

Where, θ is volumetric water content, K *is* unsaturated hydraulic conductivity, h =water pressure head, r, z is the radial and vertical coordinates, and t is time.

The flow domain for the Modified Philip-Dunne infiltrometer and double ring infiltrometer have been represented by the axisymmetric region and for these domains all boundaries have been considered as impermeable except for the surface boundary inside the MPD and DRI, and the bottom boundary which is treated as a unit gradient boundary. For MPD the soil surface inside the tube has a time varying pressure calculated from the mass balance of the water initially poured into the tube, decreasing with time due to infiltration and for DRI the soil surface inside the inner ring and the outer ring has a constant pressure.

In case of MPD, the water level vs time data had been generated numerically for a specific soil property and specific K_{sat} value and then those data were input into the MPD software.

In case of DRI, for a specific soil property and specific K_{sat} value the cumulative inflow over time of the inner ring had been generated numerically and then from the slope of the cumulative inflow vs time graph for the steady state condition, the K_{sat} value was calculated. The K_{sat} obtained from MPD software and from cumulative infiltration vs time graph for DRI were then compared with the K_{sat} of the numerical model. The water level vs time data were generated both for both homogeneous and nonhomogeneous soil. The soil was assumed to nonhomogeneous with respect to the nonuniformity of the K_{sat} value of the soil. A model was made for two-layered soil and the K_{sat} of the top soil and the bottom soil were different. The K_{sat} of the top-soil was always kept constant which is 18cm/hr and the K_{sat} of the bottom soil varied from 5E-2 to 5E-8 m/s and the depth of top soil was kept constant which was 10cm.

RESULTS AND DISCUSSIONS

Results from field test

The following table shows the comparison of K_{sat} obtained from MPD and DRI in the field, also the time and volume of water required performing the test for these two devices:

Table 1*. Comparison between field K_{sat} obtained from MPD and DRI

Location	Modified Philip Dunne Infiltrometer			Double Ring Infiltrometer		
	K_{sat} (m/s)	Time required to perform the test(hr)	Volume of water required to perform the test (m^3)	K_{sat} (m/s)	Time required to perform the test(hr)	Volume of water required to perform the test (m^3)
1	2.1E-5	1.1	0.0032	1.1E-5	3.1	0.017
2	6.4E-6	3.0	0.0033	5.8E-6	3.6	0.0153
3	7.2E-6	1.9	0.0033	7.5E-6	2.3	0.0145
4	7E-5	0.2	0.003	6.8E-5	1.7	0.0277
5	3.5E-5	0.5	0.0036	1.25E-5	2.1	0.0164

*(Ahmed et al., 2011)

This, of course, cannot be a direct comparison because the MPD is 10 cm diameter and the DRI used consisted of 20cm diameter inner ring and 40 cm outer diameter, and therefore measures a larger infiltration '*footprint*'. It is possible that the wetting front of the DRI might have intersected the wetting front of the MPD, which would affect the result of the MPD measurements. The tests with the devices were not performed precisely at the same spot, so soil conditions could have been different. Because of these reasons there are differences in results between MPD and DRI. From the table above it is clear that the double ring infiltrometer requires a larger volume of water and a greater time than MPD.

Results from computational model

Homogeneous soil. In the numerical software two models were developed; one represented the flow domain of MPD and the other one represented the flow domain of DRI. For a specific soil property and K_{sat} value the MPD model generated the water level vs time data which were input into the MPD software to estimate the K_{sat} and the DRI model generated cumulative flow vs time data which was used to estimate the K_{sat} for that soil. For homogeneous soil these three K_{sat} values; K_{sat} that was input in the numerical model, K_{sat} estimated from MPD software and from cumulative flow are shown below.

Table2**. Comparison between the K_{sat} obtained from numerical experiment on Richards equation, an application of the MPD and DRI for homogeneous soil

K_{sat} (Richards), m/s	3E-7	7.5E-7	1.6E-6	3.8E-6	1.1E-5	4.1E-5	9.3E-5
K_{sat}(MPD), m/s	4.2E-7	9.7E-7	2E-6	4.5E-6	1.4E-5	5E-5	1.1E-4
K_{sat}(DRI), m/s	1.1E-7	1.7E-7	2.5E-7	4.2E-7	1.8E-6	2.8E-6	5.8E-6

**(Ahmed et al., 2011)

The K_{sat} obtained from MPD shows better agreement with the numerical model than DRI. The cumulative flow through the inner ring of DRI is dependent on the size of the inner ring and the outer ring (Lai and Ren, 2007). Inner ring diameter≥ 80cm produce more reliable K_{sat} values than smaller diameter (Lai and Ren, 2007). But in the numerical simulation the inner ring diameter was 20cm and the outer ring diameter was 40cm because this size of DRI is mostly used in practical. Since the size of the DRI was smaller, the K_{sat} values of the DRI were highly deviated from the actual K_{sat} value of the numerical model.

Nonhomogeneous soil. The comparison of the K_{sat} obtained from numerical experiments and MPD software for nonhomogeneous soil has been shown in Table3. The depth of the top soil was 10cm and the K_{sat} of the top soil is 18cm/hr.

Table 3. Comparison between the K_{sat} obtained from numerical experiment on Richards equation, an application of the MPD and DRI for nonhomogeneous soil. K_a is the K_{sat} value of the top soil, and K_b is the K_{sat} value of the bottom soil.

K_a / K_b	K_b (m/s)	K_{DRI} (m/s)	K_{MPD} (m/s)	K_{COMSOL} (m/s)
0.001	5E-2	5.1E-6	6.2E-5	5.3E-5
0.01	5E-3	5.1E-6	6.2E-5	5.3E-5
0.1	5E-4	4.7E-6	6.1E-5	5.2E-5
1	5E-5	3E-6	6.06E-5	5E-5
10	5E-6	8.3E-7	5.9E-5	4.6E-5
100	5E-7	1.9E-7	5.8E-5	4.5E-5
1000	5E-8	3.9E-8	5.7E-5	4.4E-5

When coarse textured soil underlies fine textured soil, a low matric potential at the wetting front will prevent the water to move to the larger pore. The water will not enter into the large pores until sufficient pressure has been developed (Jury and Horton, 2004) and during the build up of this pressure the water to move laterally. In case of DRI since the model had been simulated till the flow reach steady state it involves sampling a larger volume of top-soil that is allowing the lateral flow of water than the MPD in the infiltration process. For this reason the top-soil governs the effective K_{sat} value for DRI. When a fine textured soil underlies a coarse textured soil the infiltration rate reduces directly due to the low permeable soil layer (Jury and Horton, 2004). Because DRI captures the hydraulic properties of a large volume of soil and the volume of bottom soil is larger than that of top-soil, when the low permeable soil underlies a high permeable soil the bottom soil dominates the effective K_{sat}.

The MPD infiltrometer, however, is designed to measure only the hydraulic conductivity of the top 50 cm of media and does not typically detect a confining layer below 20 cm depth. Since the depth of top-soil in this study is high, the effective K_{sat} obtained from MPD is not much affected by the K_{sat} of the bottom soil.

CONCLUSIONS

MPD infiltrometer has been used in rain gardens, infiltration basin and vegetative swales. Since this device can estimate the K_{sat} of the soil surface, it is effective for detecting the infiltration effect of fine particle accumulation on the soil surface, which is a common problem for many stormwater BMPs. The MPD software estimates the K_{sat} and the soil

suction at the wetting front. These soil properties can be used in Green-Ampt model to determine the infiltration capacity the practice for a design storm. Since the device is not heavy and requires less volume of water it is suitable to carry to the field. Because of the spatial variation of K_{sat} in the soil surface it is recommended to take a number of measurements to estimate a representative infiltration capacity of soil/media. The MPD calculations also show good agreement with the computational modal for both homogeneous and non-homogeneous soil.

ACKNOWLEDGEMENT

A special thanks to the Minnesota Pollution Control Agency, the Minnesota Local Road Research Board and Minnesota Department of Transportation.

REFERENCES

Ahmed F., Gulliver J.S. (2010). Manual for the Modified Philip-Dunne (MPD) Infiltrometer. St. Anthony Falls Laboratory (http://www.safl.umn.edu).

Ahmed F., Gulliver J. S., Nieber J. L. (2011). Rapid Infiltration Measurement of LID Best Management Practices, World Environmental Water resources & Congress conference paper (submitted).

Ashraf, M.S., B. Izadi, and B. King. (1997). Transport of bromide under intermittent and continuous ponding conditions. J. Environ. Qual. 26:69–75.

Asleson B. C., Nestingen R. S., Gulliver J. S., Hozalski R. S., Nieber J. L. (2009), Performance assessment of rain gardens, Journal of American Resource Association 45(4):1019-1031. DOI: 10.1111／j.1752-1688.2009.00344.x

Ben-Hur, M., and S. Assouline. (2002). Tillage effects on water and salt distribution in a Vertisol during effluent irrigation and rainfall. Agron. J. 94:1295–1304.

COMSOL (2010). COMSOL Multiphysics Users Guide. Version 3.5 Documentation.

Dirk, S.M., D.A. Carlson, D.S. Cherkauer, and P. Malik. (1999). Scale dependency of hydraulic conductivity in heterogeneous media. Ground Water 37:904–919.

Hanna O. T., Sandall O.C. (1995). Computational Methods in Chemical Engineering, Prentice Hall PTR.

Jury W.A., Horton R. (2004), Soil Physics, John Wiley & Sons, Inc.

Klute, A. (1986). Methods of Soil Ananlysis, Part I. Physical and Mineralogical Methods, 2nd edition. Soil Science Society of America, Inc. Publisher, Madison, WI.

Lai J., Ren L. (2007), Assessing the Size Dependency of Measured Hydraulic Conductivity Using Double-Ring Infiltrometers and Numerical Simulation

Munoz-Carpena, R., C. M. Regalado, J. Alvarez-Benedi, and F. Bartoli. (2002). Field evaluation of the new Philip-Dunne permeameter for measuring saturated hydraulic conductivity. Soil Science 167:9-24.

Nestingen R. S. (2007). The Comparison of Infiltration Devices and Modification of the Philip-Dunne Permeameter for the Assessment of Rain Gardens. Masters Thesis, University of Minnesota, Minneapolis, MN.

Philip, J. R. (1993), Approximate Analysis of Falling-Head Lined Borehole Permeameter. Water Resources Research 29:3763-3768.